Water SA 51(3) 288–301 / Jul 2025
https://doi.org/10.17159/wsa/2025.v51.i3.4135

Research paper

Removing an antibiotic from aqueous solution using sepiolite-rich dolomite – kinetic, isotherm, and thermodynamic studies

Eyüp Sabah[1], Nazile Bilgin[1] and Emine Bulut[2]

[1]*Department of Mining Engineering, Faculty of Engineering, Afyon Kocatepe University, 03200 Afyonkarahisar, Türkiye*
[2]*Department of Food Processing, Bolvadin Vocational School, Afyon Kocatepe University, 03300 Afyonkarahisar, Türkiye*

The adsorptive removal of the antibiotic drug amoxicillin (AMX) from aqueous solutions was investigated using sepiolite-rich dolomite, a cheap and natural adsorbent. AMX, one of the most frequently prescribed antibiotics, can pose environmental and health risks if not adequately treated in wastewater. Sepiolite-rich dolomite is a mineral with low sepiolite content, meso/macroporous structure, large pore diameter and volume, and divalent cations, which affect its adsorption performance for AMX removal from aqueous environments. These characteristics were examined by single-component batch adsorption methods. From the results obtained, it was observed that dolomite, which is very rich in sepiolite under optimum conditions, attained a maximum AMX adsorption capacity of 123.46 mg/g. Adsorption is mainly governed by electrostatic interactions, ion exchange, and pore-filling mechanisms. It is clear that mesoporosity is the major controlling factor in sepiolite-rich dolomite in terms of sorption intensity and capacity compared to surface area. The Freundlich isotherm model and pseudo second-order kinetic model were found to be the best fit for the AMX adsorption results. Additionally, scanning electron microscope with energy dispersive X-ray spectroscopy (SEM-EDX), X-ray diffraction (XRD), and Fourier transform ınfrared spectroscopy (FTIR) analysis revealed that sepiolite-rich dolomite has a strong affinity for AMX and the adsorption of AMX is strongly influenced by exchangeable cations and molecules such as Ca^{2+} and Mg^{2+}, and H_2O in zeolite-like channels, Si-OH groups located on basal surfaces, and the open channel defects (OCD) in its structure.

CORRESPONDENCE
Eyüp Sabah

EMAIL
esabah@aku.edu.tr

DATES
Received: 19 March 2024
Accepted: 7 July 2025

KEYWORDS
amoxicillin
sepiolite-rich dolomite
adsorption
wastewater treatment

COPYRIGHT
© The Author(s)
Published under a Creative Commons Attribution 4.0 International Licence (CC BY 4.0)

INTRODUCTION

Pharmaceutical chemicals, especially antibiotics, are classified as emerging environmental pollutants, defined as resistant bioaccumulative compounds. These are hazardous and toxic chemicals (Boshir Ahmed et al., 2015). Studies have shown that wastewater treatment plants are only effective in removing 20–90% of the antibiotic residues (Perini et al., 2018). However, some antibiotics such as tetracyclines and fluoroquinolones cannot be removed from the environment because they are resistant to natural degradation (Becker et al., 2016).

Amoxicillin is a widely used antibiotic that belongs to the β-lactam group of antibiotics. It is efficient against both gram-negative and gram-positive bacteria and is commonly prescribed for treating respiratory, urinary, and skin infections (Aranda and Rivas, 2022; Narayanan et al., 2024). However, the extensive and inappropriate use of amoxicillin has led to its accumulation in the aquatic medium, posing a prominent risk to human health and ecosystems. Amoxicillin can induce bacterial resistance, inhibit the normal functioning of the microbial environment, and interfere with the endocrine system of humans and aquatic organisms (Al-Gheethi and Ismail, 2014; Hughes et al., 2016; Gomes, 2024). Therefore, it is necessary to remove AMX appropriately and economically from wastewater before discharge. Among the various methods available for degrading and removing AMX from home and/or industrial wastewater are adsorption using different kinds of adsorbents (Khumalo et al., 2023; Mohammed et al., 2024; Abbas and Trari, 2024; Putra et al., 2009; Mansouri et al., 2015; Pezoti et al., 2016; De Franco et al., 2017; Sellaoui et al., 2017; Güngördü, 2018; Özer, 2020; Imanipoor et al., 2021), ozonation (Li et al., 2014; Silva et al., 2022), biodegradation (Liu et al., 2015), advanced oxidation processes (AOPs) (Kıdak and Doğan 2018; Wang et al., 2023), membrane filtration (reverse osmosis-ultrafiltration (RO-UF)) (Nasrollahi et al., 2022; Gholami et al., 2012), nanofiltration (Homayoonfal and Mehrnia, 2014), and photocatalytic degradation (Liu et al., 2024; Javed et al., 2025). Technologies such as ozonation and enhanced oxidation cause the formation of unwanted toxic by-products during the treatment of antibiotics. Adsorption is noted as one of the most promising techniques because of its high yield, low cost, and simple process across a wide concentration range.

However, the fundamental challenge in applying adsorption techniques is selecting a suitable/efficient adsorbent. Until this time, different natural/synthetic adsorbents such as bentonite, activated carbon, magnetic graphene oxide, kaolinite, organoclay, carbon nanotubes, porous polymers, zeolite, and zero-valent iron nanoparticles have been utilized to remove AMX from water and wastewater by adsorption (Anastopoulos et al., 2020). Among them, activated carbon is the favoured adsorbent because of its porosity, adsorption capacity, and high specific surface area; yet, its usage is limited due to its high cost when applied on a large scale. Investigators have thus focused their attention on inexpensive, natural, environmentally benign, economical, and readily available adsorbents.

Despite their low cost, mechanical and chemical stability, surface and structural characteristics/diversity, and high surface area, investigations on removing AMX from water and wastewater using clay minerals have remained very limited (Putra et al., 2009; Maia et al., 2017; Yeo et al., 2024).

Sepiolite is a naturally occurring clay mineral belonging to the phyllosilicates group. Due to its properties, such as micropores and zeolitic channels that constitute its internal structure and contribute a high surface area, and the fact that these properties can be modified/enhanced by thermal and/or acid activation or long-chain quaternary ammonium cations, sepiolite is increasingly used in sorption processes. Sepiolite-rich dolomite differs from dolomitic sepiolite and sepiolite in terms of physical, chemical, mineralogical, and textural characteristics. The sepiolite-rich dolomite is composed of <20% sepiolite and > 80% dolomite, whereas, dolomitic sepiolite consists of 20–40% dolomite, while sepiolite clay comprises >80% sepiolite. Sepiolite-rich dolomite has the lowest surface area and the highest unit volume weight due to its high dolomite content. Notably, sepiolite-rich dolomite offers a significant cost advantage, at approximately 10% of dolomitic sepiolite and 5% of sepiolite clay.

Unlike activated carbon, clays, and nanomaterials, the application of sepiolite-rich dolomite in AMX removal has not been previously reported in the literature. This study not only addresses this gap but also emphasizes the unique properties of sepiolite-rich dolomite, including its micro/mesoporous structure, surface area, and economic advantages, which distinguish it from other adsorbents. This work comprehensively investigates adsorption mechanisms through detailed mineralogical/physicochemical characterization and adsorption performance evaluations, providing fundamental insights into the processes governing AMX removal. Furthermore, advanced analyses, such as Fourier transform infrared spectroscopy (FTIR), energy dispersive X-ray spectroscopy (EDX), scanning electron microscopy (SEM), and X-ray diffraction (XRD), were employed to systematically characterize the adsorbent's surface properties and morphology before and after adsorption, offering new insights into its functional properties.

MATERIALS AND METHODS

Materials

Sepiolite-rich dolomite was collected from the Upper Sakarya Formation (Kurtşeyh-Sivrihisar, Turkey), located within the Central Anatolian Neogene Basins. The sample had a moisture content of about 40% in its original state.

The adsorbate used in this study was amoxicillin trihydrate (Table 1), which is non-hygroscopic. The stable solid form was obtained from Atabay Chemical Industry Trade Inc. (Istanbul, Turkey). A primary stock solution of AMX trihydrate at 1 000 mg/L was prepared by dissolving an appropriate amount in DI water. Because exposure to sunlight can cause degradation, the prepared amoxicillin solutions were consumed in a short time in experimental studies, and were stored in the refrigerator when not in use. Working solutions were prepared at average intervals of 4–5 days. Sigma-Aldrich quality NaOH and HCl were utilized to adjust pH. All experiments employed deionized (DI) water with a conductivity of 0.055 µS/cm.

Preparation of adsorbent

After drying in an oven, the sample of the raw sepiolite-rich dolomite was broken down in two stages using a laboratory jaw and a roller crusher, reducing its particle size to below 2 mm. It was then ground in a vibrating ball mill to obtain a suitable size for adsorption experiments. Particle size distributions of the samples ground in the previous stage were obtained using the laser light scattering technique with the Malvern Mastersizer 2000 brand device (Malvern Instruments Ltd., Malvern, UK).

Characterization of adsorbent

The raw sepiolite-rich dolomite was analysed using an X-ray fluorescence (XRF) spectrometer (ZSX Primus II XRF, Rigaku Corporation, Tokyo, Japan) and an X-ray diffractometer (XRD) (Panalytical X Pert Pro MPD, PANalytical B.V., Almelo, The Netherlands) to determine its mineralogical and chemical compositions. Its density was determined by Quantachrome Ultrapycnometer 1000 model helium pycnometer (Boynton Beach, USA). The cation ratios for the raw sepiolite-rich dolomite were computed based on 33 oxygen molecules (Jones and Galan, 1988) per half-unit cell and by employing the molecular quantities of oxygen-containing compounds from chemical analysis data. A LEO 1430 VP model scanning electron microscope (LEO Electron Microscopy Ltd., Cambridge, UK) equipped with an energy-dispersive X-ray spectrometer (EDX) was used for evaluating the morphological and textural properties of raw and AMX adsorbed sepiolite-rich dolomite samples. Qantachrome analyzer (Quantachrome, Ltd., Hook, Wales, UK) using nitrogen gas adsorption at −196°C was utilized to measure mean pore diameter, pore volume, and the BET surface area. The DFT (density functional theory) analysis was utilized to characterize the pore structure and specific pore volume of the sepiolite-rich dolomite samples. DFT is a statistical thermodynamic approach that models the adsorption and desorption processes in porous materials. The theory assumes that adsorption occurs in pores of varying sizes and shapes, and pore size distributions are calculated based on equilibrium adsorption isotherms. The nitrogen adsorption isotherm data were analysed using the DFT model to obtain cumulative pore volume and differential pore volume curves as a function of pore half-width. $dV/(r)$ is obtained by calculating the numerical derivative of cumulative pore volume concerning pore half-width at each corresponding point. The raw and AMX adsorbed sepiolite-rich dolomite samples were analysed using Fourier transform infrared spectroscopy (FTIR) on the IRAffinity-1 CE (Shimadzu, Kyoto, Japan) over the spectral range of 4 000 and 400 cm^{-1} (32 scans, 4 cm^{-1} resolutions). Prior to FTIR analysis, the sample-to-KBr ratio was maintained at 1:100 (w/w), and the disks were pressed under 25 N/mm^2 pressure for 2 min.

Table 1. Physicochemical properties of amoxicillin trihydrate (Baghapour et al., 2014)

	Structure	Chemical formula	Molar mass (g/mol)	Polar surface area (Å$^{2)}$)	Water solubility at 25°C (mg/L)
Amoxicillin trihydrate	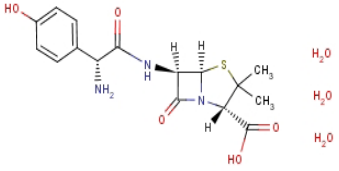	$C_{16}H_{19}N_3O_5S{\cdot}3H_2O$	419.55	161	3 430

Measurement of the zeta potential of raw sepiolite-rich dolomite as a function of pH was determined at 23±5°C with the Zetasizer Nano-Z (Malvern Instruments Ltd., Malvern, UK) device using the microelectrophoresis/electrophoretic light scattering technique. In this process using a magnetic stirrer, sepiolite-rich dolomite suspensions with a minimum solid concentration of 0.1 g/L, containing 10^{-3} M KCl (inert electrolyte), were stirred at 500 r/min to prevent interactions between particles (10^{-2}% mass according to Malvern's guideline). The suspension pH values were adjusted using 0.1 M HCl or NaOH solutions. The pH of the solution was measured by using the HI 1131 pH electrode with the Ag/AgCl reference cell HI5522 Digital, bench-model pH-ISE-conductivity meter (Hanna Instruments Inc., Woonsocket, Rhode Island, USA). At the end of the 10-min conditioning, the suspensions were centrifuged at 3 000 r/min for an additional 10 min, and a sample was taken from the supernatant to determine the zeta potential values. An average of 10 measurements was taken to represent the measured potential.

Batch experiments for AMX removal

The equilibrium adsorption studies were performed by batch technique in various concentrations of AMX (12.5, 25, 50, 75, 100, 150, 200 mg/L) and sepiolite-rich dolomite dosages (1, 3, 5, 7, 10, 20 g/L) at different contact times (2.5, 5, 10, 15, 30, 60 min) and temperatures (25, 35, 45, 55°C). The suspensions were prepared in 25 mL screw-capped PP centrifuge tubes. The mixing processes were carried out in a GFL 1086 brand thermostatic shaking water bath (Burgwedel, Germany) with orbital movement at a constant mixing speed of 250 r/min at the desired pH, temperature, and contact times. After mixing, the suspensions were centrifuged with a Hettich Universal 32 centrifuge for 10 min at 7 000 r/min (Hettich GmbH and Co. KG, Tuttlingen, Germany). Then, aliquots were taken from the clear part of the suspension, and the equilibrium concentration of the adsorbate was evaluated by the UV-spectrophotometric method. UV-spectrophotometric measurements were carried out at 229 nm with a Thermo Scientific Multiskan GO Microplate spectrophotometer (Thermo Fisher Scientific, Vantaa, Finland). The difference between the initial and final concentrations of AMX was calculated as the amount adsorbed on the solid surface (q_e) by using Eq. 1, and the maximum adsorption density (Γ_m) was computed by dividing q_e by the specific surface area of the adsorbent (m^2/g) using Eq. 2.

$$q_e = \frac{(C_i - C_e)V}{W} \quad (1)$$

$$\Gamma_m = \frac{(C_i - C_e)V}{WS \times 1000} \quad (2)$$

Here, C_e and C_i (mg/L) are equilibrium and initial concentrations of AMX, respectively. W (g), Γ_m (mol/m^2), S (m^2/g), and V (L) are mass of the adsorbent, the maximum adsorption density, the specific surface area of the adsorbent, and the volume of the solution, respectively.

RESULTS AND DISCUSSION

Characterization of sepiolite-rich dolomite

The micronized product obtained from the dry grinding of sepiolite-rich dolomite had a narrow size distribution, with 98% of the particles being smaller than 104 µm and a mean diameter (d_{50}) of 12.08 µm.

XRD analysis

The X-ray diffraction results for sepiolite-rich dolomite, which shows its semi-quantitative mineralogical compositions, is presented in Fig. 1, and its relevant physical, physicochemical, and chemical properties are given in Table 2. The XRD diagram indicates that dolomite is the dominant mineral, with characteristic 2θ-diffraction peaks observed at 24.04, 30.94, 41.13, and 50.53 degrees, corresponding to the (012), (104), (113), and (018) planes of the $CaMg(CO_3)_2$ structure, respectively (JCPDS card no. 36-0426) (Xie et al., 2016). Sepiolite is the second-most abundant mineral, followed by minor impurities of calcite and quartz, corresponding to ~2%. The chemical analysis confirms this, with CaO content at 20.94%, and LOI at 34.88%, indicating that the sepiolite-rich dolomite is a low-rank sepiolite (Alver et al., 2008). The structural composition of sepiolite-rich dolomite (Table 3) was derived from the chemical analysis data using the molecular quantities of oxygen-containing compounds. The Ca/Mg ratio of sepiolite-rich dolomite is 0.71, confirming that the main mineral is dolomite. Karakaya et al. (2004) ascribed the presence of the main carbonate mineral to dolomite where the Ca/Mg ratio of the layers is <1.60. It is seen that Mg^{2+} ions are dominant in the octahedral sheet, and there are also small amounts of Al, Fe^{3+}, and very little Ti. The intermediate layer cations of Na^+, K^+, and Ca^{2+} are very high (6.54) (Table 3).

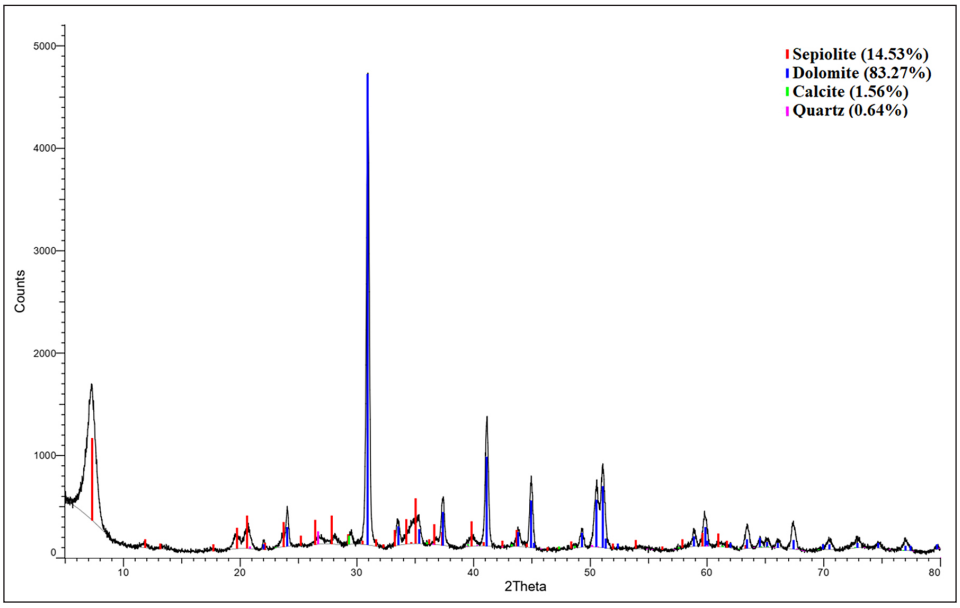

Figure 1. X-ray diffraction patterns of the sepiolite-rich dolomite

Table 2. The characteristics of sepiolite-rich dolomite

Characteristics	Sepiolite-rich dolomite
Composition (wt %):	
SiO_2	21.08
Al_2O_3	0.59
Fe_2O_3	0.32
CaO	20.94
MgO	21.06
Na_2O	0.02
K_2O	0.07
TiO_2	0.04
LOI	34.88
Colour	white
Moisture (%)	7
Density (g/cm^3)	2.57
BET surface area (m^2/g)	141
Average pore diameter (Å)	77.6
Total pore volume (cm^3/g)	0.251
Zeta potential at natural pH 7.92 (mV)	–18.1

Table 3. Structural composition calculated of sepiolite-rich dolomite

Sheets/elements	Cation ratios
Tetrahedral sheet:	
Si	6.15
Octahedral sheet:	
Mg	9.16
Al	0.20
Fe^{3+}	0.07
Ti	0.009
Interlayer:	
Ca	6.54
Na	0.01
K	0.003

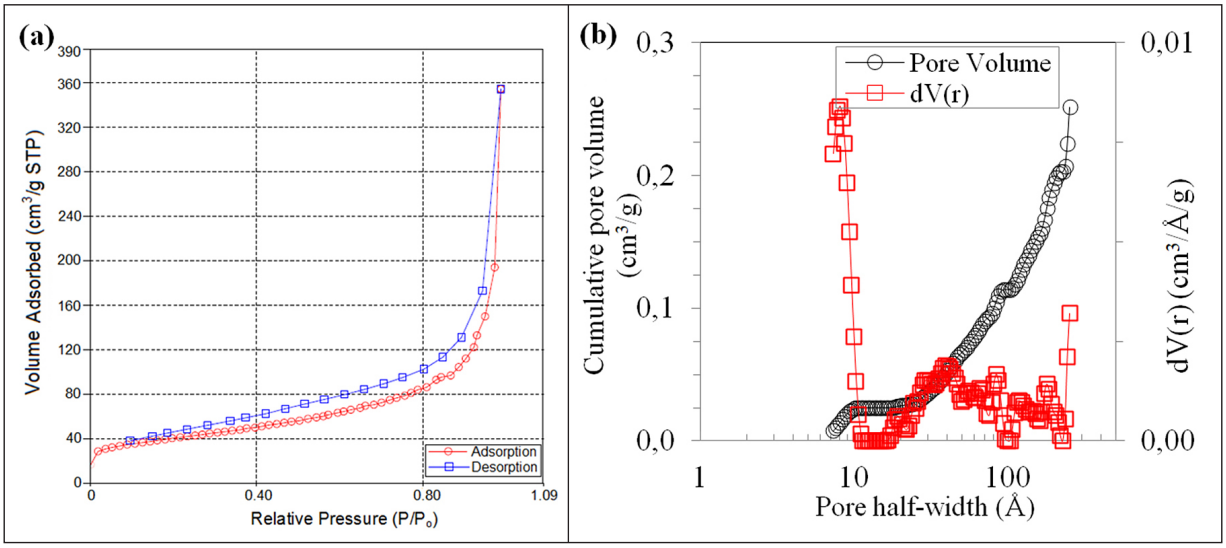

Figure 2. (a) N_2 adsorption desorption isotherms of sepiolite-rich dolomite at 77 K and (b) specific pore volume and pore size distribution for sepiolite-rich dolomite

BET analysis

Figure 2a depicts the N_2 adsorption-desorption isotherms of sepiolite-rich dolomite used as an adsorbent at 77K, while Fig. 2b depicts the pore diameter-dependent log-differential pore volume and pore size distribution curves. The isotherm curves conform to Type IV isotherms and have an H3-type hysteresis loop, according to the IUPAC (International Union of Pure and Applied Chemistry) classification (Chuaicham et al., 2019; Mohammed and Alnasrawi, 2024). The H3-type hysteresis loop shows a mesoporous system with an interwoven network structure and a structure consisting of macropores that are not entirely filled with pore network pore condensation (Liu et al., 2015). However, the fact that it holds less nitrogen gas at low relative pressure ($P/P_0 < 0.40$) (micropore filling) indicates that sepiolite-rich dolomite has a more macroporous structure. In addition, at high relative pressures ($P/P_0 > 0.40$), due to the effect of multilayer adsorption and capillary condensation, the hysteresis loop is formed (Figueiredo et al., 2024), and the bending between 0.2 and 0.9 (P/P_0) does not follow a course parallel to the relative pressure axis. This situation indicates that the porous network consists of narrow pores opening into wider ones and/or that there is a significant presence of mesopores as well as micropores. Moreover, the narrow hysteresis loop observed at $P/P_0 > 0.9$ implies that sepiolite-rich dolomite has wide mesopores (Sun et al., 2022; Yang et al., 2024). The specific pore volume and log-differential size distribution curves found with the DFT (density functional theory) technique from the adsorption isotherm data (Fig. 2b) also confirm this situation.

From the pore size distribution graph of sepiolite-rich dolomite (Fig. 2b), pore openings are between 7 and 251 Å (0.7–25.1 nm), average pore diameter is 19.7 Å (1.97 nm), and pore volume is 0.251 cm^3/g. The average pore opening determined from the surface area and specific micro-mesopore volume of sepiolite-rich dolomite is 7.76 nm. These data confirm that the specific surface area of sepiolite-rich dolomite is 141 m^2/g. It is reported in the literature that the BET-specific surface areas of high-quality sepiolites of Sivrihisar/Polatlı-Eskişehir origin vary from 243 m^2/g (Uğurlu, 2009) to 342 m^2/g (Alkan et al., 2007), with 330 m^2/g the most common value (Lescano et al., 2014). The high specific surface area values are associated with the structural channels (or tunnels) that characterize the specified mineral, especially its fibrous morphology, micronized grain, and ground particle size. Considering all these aspects, it can be said that the sepiolite-rich dolomite with a lower surface area has a more long-fibred and open-textured morphological structure.

SEM-EDX analysis

The SEM images of the fibres of sepiolite-rich dolomite show bundles and/or rods due to the dry grinding process (Bastida et al., 2006; Yang et al., 2024). The sepiolite fibres with a net-like structure surrounding the dolomite indicate that these minerals may very well have developed together (Yalçın and Bozkaya, 2004). The semi-quantitative EDX analysis data (Fig. 3) show that the sepiolite-rich dolomite is mainly composed of Mg and Si, with major amounts of Ca and minor amounts of Al. Accordingly, the EDX analysis results of the sepiolite-rich dolomite confirm the chemical analysis results given in Table 2.

FTIR analysis

Figure 4a shows the FTIR spectrum of raw sepiolite-rich dolomite obtained before adsorption in the 4 000–400 cm^{-1} wavelength range. Accordingly, a less intense Mg_3OH band is formed in the 3 564–3 690 cm^{-1} region due to the stretching vibrations of the OH– groups in the octahedral sheet and on the surface (Walczyk, 2020). A weak band is observed at 3 406 cm^{-1} due to the H–O–H vibrations of the adsorbed water (Wu et al., 2017). Additionally, the weak bands at 1 654 cm^{-1}, which develop because of the OH-bending vibration, reflect the relative water deformation in the Mg-coordination and the OH-stretching of the zeolitic water located in the channel cavities (Zhang et al., 2023). The deep bands seen at 1 450 cm^{-1}, 880 cm^{-1}, and 730 cm^{-1} in the FTIR spectrum of raw sepiolite-rich dolomite are very intense peaks originating from dolomite and other carbonates (Suárez et al., 2016). The weak peaks in the 470–650 cm^{-1} region are because of the OH groups attached to the Mg^{+2} ions in the octahedral sheet and the SiO-bending vibrations in the tetrahedral sheet (Lescano et al., 2014).

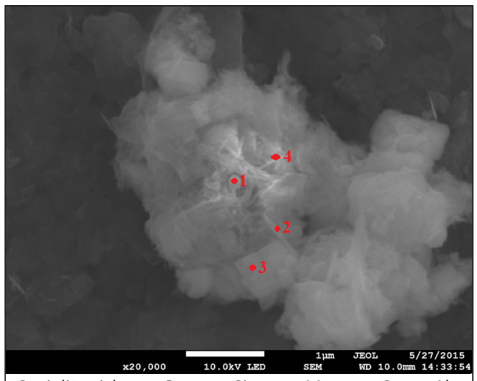

Sepiolite-rich dolomite	O	Si	Mg	Ca	Al
Pt-1	41.76	5.09	14.62	24.61	0.12
Pt-2	40.38	2.70	14.54	24.84	-
Pt-3	41.15	2.20	14.28	23.71	-
Pt-4	37.27	2.62	9.74	14.21	-
$\sum_{n=1}^{n} P_t/n$	40.14	3.15	13.30	21.85	0.12

Figure 3. Representative SEM image and EDX analysis of sepiolite-rich dolomite

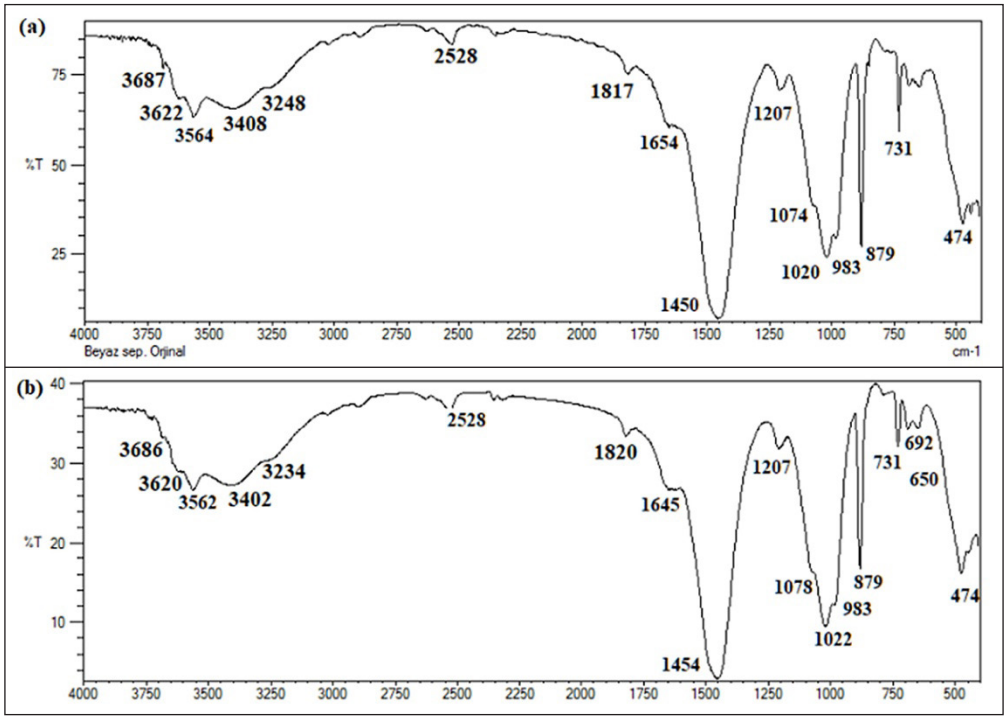

Figure 4. FTIR spectrum of (a) the raw sepiolite-rich dolomite before and (b) the raw sepiolite-rich dolomite after amoxicillin adsorption

AMX adsorption onto sepiolite-rich dolomite

The adsorption isotherm curve of amoxicillin on sepiolite-rich dolomite at 25°C, which represents the equilibrium distribution of the adsorbate on the adsorbent, is displayed in Fig. 5. The adsorption capacity of sepiolite-rich dolomite was very high, indicating that amoxicillin had a strong and uniform affinity for the adsorbent. Adsorption capacity increased linearly as the initial amoxicillin concentration (C_0) increased from 0 to approximately 150 mg/L, reaching 76.23 mg/g. Corresponding to this C_0 range, the equilibrium concentrations of amoxicillin (C_e) ranged from 0 to 73.77 mg/L. When C_0 values increased from 150 to 200 mg/L, the adsorption capacity showed a sharp increase, reaching a maximum value of 114.97 mg/g, while the corresponding Ce values ranged from 73.77 to 85.03 mg/L. The trend of the isotherm curve exhibits a C1-type behaviour at low concentrations and an S1-type behaviour at high concentrations, in accordance with the Giles classification (Giles et al., 1974), indicating the heterogeneity (Dabrowski, 1986) of the sepiolite-rich dolomite surface and the competition between the AMX and the solvent molecules. For such an isotherm to occur, the adsorbent must have a porous structure containing flexible molecules and different crystal regions and must interact more with the solute molecules than the solvent molecules (Hinz, 2001).

The adsorption isotherm for AMX onto sepiolite-rich dolomite (Fig. 5) indicated that the adsorption process was influenced by the heterogeneity and porosity of the adsorbent surface. To further elucidate the adsorption process and determine adsorbent/adsorbate interactions, various kinetic models, such as pseudo-first-order, pseudo-second-order, and intraparticle diffusion models, were adapted to the empirical data.

The pseudo-first-order model assumes that adsorption occurs on a single class of sites and is proportional to the number of unoccupied sites, given in Eq. 3:

$$q_t = q_e(1 - e^{-k_1 t}) \quad (3)$$

where q_t is the amount of solute adsorbed at time t, q_e is the equilibrium adsorption capacity, and k_1 is the rate constant. The pseudo-second-order model assumes chemisorption as the rate-limiting step (Eq. 4):

$$q_t = \frac{k_2 q_e^2 t}{1 + k_2 q_e t} \quad (4)$$

where k_2 is the rate constant of pseudo-second-order adsorption.

The mathematical equations of the kinetic models were utilized to fit the empirical results of the AMX adsorption capacity of sepiolite-rich dolomite as a function of contact time. The adsorption rate is assumed to be proportional to the difference between the equilibrium and actual adsorption capacities in the pseudo-first-order model. In contrast, in the pseudo-second-order model, it is assumed that the adsorption rate is proportional to the square of this difference. Table 4 gives the parameters of these models, the correlation coefficients (R^2), equilibrium adsorption capacities ($q_{m(cal)}$ and $q_{m(exp)}$), and rate constants (k_1 and k_2).

The suitability of the models was evaluated by comparing the theoretical value calculated from the kinetic model ($q_{m(cal)}$) with the experimental value ($q_{m(exp)}$) and by examining the linear regression coefficient (R^2). According to the results, the pseudo-second-order model better fits the data than the pseudo-first-order model, as indicated by the higher R^2 values and the closer agreement between $q_{m(cal)}$ and $q_{m(exp)}$. This means that the adsorption of AMX on sepiolite-rich dolomite is influenced by multiple factors, including surface adsorption, intraparticle diffusion, and intrapore liquid film diffusion. Similar results were reported by Putra et al. (2009) using bentonite adsorbent, by Chayid and Ahmed (2015) and Pezoti et al. (2016) using activated carbon prepared from biomass adsorbent for AMX adsorption, and by Balarak et al. (2020) using surfactant-modified sepiolite adsorbent for ciprofloxacin removal. In terms of investigating the diffusion process, the intraparticle diffusion model was also applied for the adsorption of AMX to sepiolite-rich dolomite (Fig. 6). This model assumes that the adsorption rate is controlled by the diffusion of the adsorbate molecules from the bulk solution to the pores of the adsorbent, which can be expressed as $q_t = k_p t^{1/2} + C$. Here, C is a constant related to the boundary layer thickness, k_p is the intraparticle diffusion rate constant (mg/(g·min$^{-1/2}$)), and q_t is the amount of AMX adsorbed at time t (mg/g). The graph of q_t versus $t^{1/2}$ should give a straight line with an intercept of C and a slope of k_p. If the plot passes through the origin, it indicates that intraparticle diffusion is the sole rate-limiting step.

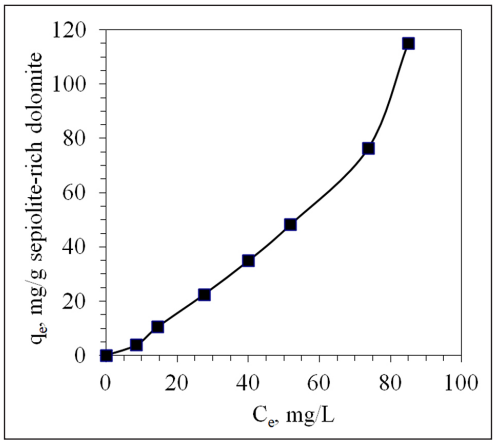

Figure 5. AMX adsorption isotherm on sepiolite-rich dolomite at 25°C (C_0: 12.5 to 200 mg/L, pH: 3, t: 30 min, m: 1 g/L)

Table 4. Parameters and correlation coefficients of pseudo-first-order and pseudo-second-order kinetic models for the adsorption of AMX on using sepiolite-rich dolomite (C_0: 50 mg/L, T: 25°C, pH: 3, m: 1 g/L, N: 250 r/min)

Pseudo-first-order				Pseudo-second-order			
k_1 (min^{-1})	$q_{m(cal)}$ (mg/g)	$q_{m(exp)}$ (mg/g)	R^2	k_2 (g/(mg·min))	$q_{m(cal)}$ (mg/g)	$q_{m(exp)}$ (mg/g)	R^2
0.254	23.75	23.58	0.814	0.218	23.64	23.58	0.9999

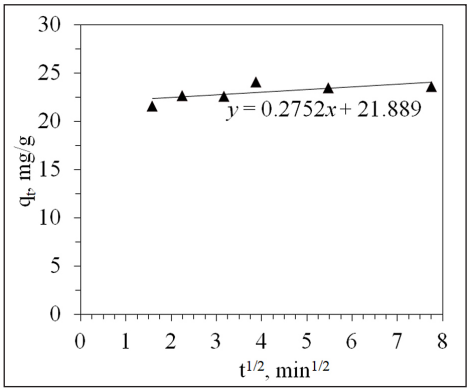

Figure 6. Plot of intraparticle diffusion kinetic model for AMX adsorption by sepiolite-rich dolomite

Table 5. Obtained parameters of the intraparticle diffusion model for AMX adsorption on sepiolite-rich dolomite

k_p (mg/(g·min$^{-1/2}$))	R^2	C (mg/g)
3.64	0.4948	21.89

However, the fact that the plot does not pass through the origin indicates that intra-particle diffusion is not the only controlling process, and others, such as external mass transfer or surface reaction, may also influence the adsorption rate (Wang and Guo, 2022).

The factors of the intraparticle diffusion model for AMX adsorption on sepiolite-rich dolomite are given in Table 5 as k_p = 3.64 mg/(g·min$^{-1/2}$), R^2 = 0.4948, and C = 21.89 mg/g. The results also show that the plot of q_t versus $t^{1/2}$ does not pass through the origin (Fig. 2) and has a low R^2 value, indicating that intraparticle diffusion is not the sole rate-limiting step for AMX adsorption on sepiolite-rich dolomite. According to the Weber-Morris intraparticle diffusion model, the constant C, which represents the boundary layer effect, is indicative of the extent to which film diffusion influences the overall adsorption kinetics. A non-zero C value implies that the adsorption process is not solely governed by intraparticle diffusion but also involves significant contributions from film diffusion (Dharmarathna and Priyantha, 2024). In the current study, the C value obtained was 21.89 mg/g, suggesting that external mass transfer resistance due to the boundary layer plays a critical role in adsorption. This aligns with the findings of Wu et al. (2009) and similar studies (Song, 2018; Balarak et al., 2020) which state that when the intercept C is non-zero, both intraparticle diffusion and film diffusion occur simultaneously as rate-controlling steps. The high C value also points to differences in mass transfer rates during the initial and later stages of adsorption, indicating a sequential mechanism where film diffusion dominates initially, followed by intraparticle diffusion.

This result is consistent with the fact that sepiolite-rich dolomite has a more macroporous than microporous structure, as shown with the nitrogen adsorption-desorption isotherm data given in Fig. 2. A macroporous structure implies that the adsorbent has a large pore volume and a wide range of macropores (d > 500 Å) and pore sizes (20 < d < 500 Å), which can facilitate the adsorption of large molecules such as amoxicillin. A macroporous structure also implies that the adsorbent has a low BET-specific surface area, as reported by Hussaini and Dvorkin (2021), which indicates that it has a small number of active sites for adsorption (Mane et al., 2024; Zhang et al., 2024). Therefore, the fact that sepiolite-rich dolomite has a more macroporous structure (pore volume 0.251 cm^3/g; pore size 77.6 Å) than a microporous one is likely responsible for the high value of its pseudo-second-order rate constant (k_2), confirming the presumption of the significance of vacant sites for a pseudo-second-order process.

Adsorption equilibrium and capacity under different conditions were also investigated. The experimental data were fitted to the Langmuir (Eq. 5) and Freundlich (Eq. 6) models. The Langmuir isotherm assumes that adsorption occurs on a surface with a finite number of equivalent and homogeneous adsorption sites, where each site can hold only one molecule (monolayer adsorption). It assumes no interaction between adsorbed molecules. The nonlinear form of the Langmuir equation is:

$$q_e = \frac{q_m K_L C_e}{1 + K_L C_e} \quad (5)$$

where C_e and q_e indicate the equilibrium concentration of solute (mg/L) and the amount of solute adsorbed per unit mass of adsorbent (mg/g), respectively. K_L and q_m are the Langmuir constant (L/mg) related to the adsorption energy and the maximum adsorption capacity, respectively.

The Freundlich isotherm describes adsorption on heterogeneous surfaces with varying adsorption energies. It assumes that adsorption capacity increases with increasing solute concentration but at a decreasing rate. The nonlinear form of the Freundlich equation is:

$$q_e = K_F C_e^{1/n} \quad (6)$$

where K_F ((mg/g)(L/mg)$^{1/n}$) is the Freundlich equation constant indicating adsorption capacity, and n is a dimensionless constant representing adsorption intensity of surface heterogeneity (Foo and Hameed, 2010).

The linearized Langmuir and Freundlich adsorption isotherms for AMX onto sepiolite-rich dolomite at 25°C are shown in Fig. 7 and the corresponding isotherm constants derived from the plots are presented in Table 6. Based on the correlation coefficients, the Freundlich model demonstrates a better fit compared to the Langmuir model.

The maximum adsorption capacity of 123.45 mg/g on sepiolite-rich dolomite/AMX at 25°C was comparable to or higher than that reported for other low-cost adsorbents (Table 7). The Freundlich constant of n = 0.7247, which is less than 1, indicates a cooperative adsorption mechanism where the adsorption sites become increasingly favourable as more AMX molecules are adsorbed. This is consistent with S-type isotherms, suggesting an enhancement in adsorption affinity due to intermolecular interactions among AMX molecules on the adsorbent surface. Such behaviour highlights the heterogeneous nature of the sepiolite-rich dolomite surface and supports the multilayer adsorption characteristics predicted by the Freundlich model (Saadi et al., 2015). Moreover, the n value being less than 1 could be an indication of physical adsorption (Gündüz and Bayrak, 2017). However, this alone is insufficient to definitively classify the adsorption type as physical or chemical. Thermodynamic parameters, such as adsorption enthalpy or enthalpy changes, are essential for determining the precise nature of the adsorption process.

As shown in Fig. 8, the adsorption isotherms indicate that q_e increases nonlinearly with C_e at all temperatures, reflecting the heterogeneous nature of the sepiolite-rich dolomite surface (López-Luna et al., 2019). This indicated that the adsorption sites on the sepiolite-rich dolomite surface were not equally accessible or favourable for AMX molecules and that some degree of interaction or repulsion occurred between the adsorbed layers. The trend of the curves varied with temperature between 25 and 45°C, suggesting that adsorption equilibrium is only slightly influenced by temperature in this range. However, at 55°C, the q_e values are notably lower, particularly at higher C_e concentrations. This decline is likely due to the thermal degradation of AMX molecules at elevated temperatures (Palma et al., 2016), which reduces their availability for adsorption.

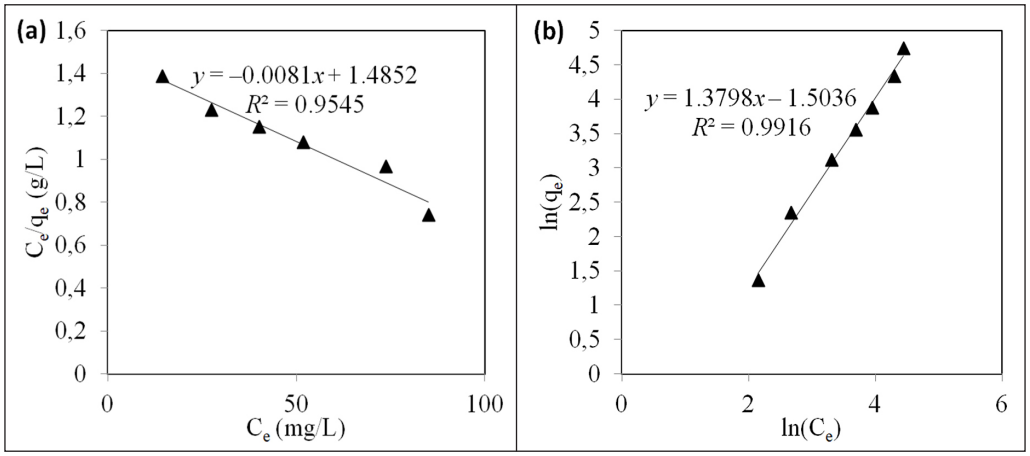

Figure 7. (a) Langmuir, and (b) Freundlich isotherm plots for AMX adsorption to beige sepiolite at 25°C

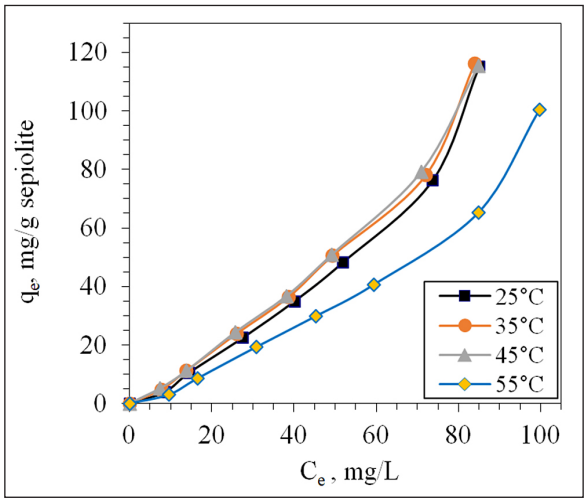

Figure 8. AMX adsorption isotherms onto sepiolite-rich dolomite at different temperatures (C_0: 12.5 to 200 mg/L, pH: 3, m: 1 g/L, *t*: 30 min)

Table 6. Langmuir and Freundlich isotherm constants at 25°C

Adsorbent	Langmuir			Freundlich		
	q_m (mg/g)	K_L (L/mg)	R^2	*n*	K_F ((mg/g)(L/mg)$^{1/n}$)	R^2
Sepiolite-rich dolomite	123.45	0.0055	0.9546	0.7247	0.2225	0.9916

Table 7. Maximum adsorption capacity (q_{max}) values of AMX in case of using different adsorbents

Adsorbent	q_{max} (mg/g)	Reference
Natural bentonite	44.66	Budyanto et al., 2008
Bentonite	53.93	Putra et al., 2009
Organo bentonite	26.18	Zha et al., 2013
Organoclays	24.39	Jin et al., 2014
Giant reed	92.10	Chayid and Ahmed, 2015
Multi-walled carbon nanotubes	22.90	Mohammadi et al., 2014
Granular AC	4.40	De Franco et al., 2017
AC800 from termite bio-waste	23.43	Niero et al., 2021
AC from jujube nuts	73.96	Belaissa et al., 2022
AC from olive stone	57.00	Limousy et al., 2017
AC nanoparticles prepared from vinewood	2.69	Pouretedal and Sadegh, 2014
AC prepared from waste citrus peel	125.00	Kam and Lee, 2018
Sepiolite-rich dolomite	123.46	This study

Understanding the nature, spontaneity, feasibility, and mechanism of the adsorption phenomenon is provided by adsorption thermodynamic parameters such as enthalpy, entropy changes, and free energy. By analysing these parameters, one can determine the driving force, the heat effect, and the disorder of the adsorption system. Thermodynamic factors of adsorption of AMX molecules on sepiolite-rich dolomite, presented in Table 8, were calculated with the Van't Hoff, Gibbs free energy, and entropy change equations.

The experimental data demonstrated that the adsorption of AMX to sepiolite-rich dolomite occurred spontaneously and exothermically in nature. The ΔG_{ads} values were negative at all temperatures, ranging from −14.44 kJ/mol at 298 K to −15.19 kJ/mol at 328 K. This indicated that the adsorption was thermodynamically favourable and driven by the decrease in free energy in the system. The value of ΔH_{ads} was also negative, at −5.86 kJ/mol, suggesting that the adsorption phenomenon wasexothermic (Sahmoune, 2019). This was consistent with the decrease in adsorption capacity with increasing temperature, as higher temperatures reduce the driving force for adsorption. The value of ΔS_{ads} was slightly positive, 0.03 kJ/(mol·K), so it can be said that the randomness at the solid-liquid interface increased in the adsorption phenomenon (Ahmet et al., 2015; Genç and Dogan, 2015). This could be because of the H_2O molecules released from the sepiolite-rich dolomite surface and the AMX hydration shell or the rearrangement of AMX molecules on the sepiolite-rich dolomite surface (Sabah and Ouki, 2017; Prabhu and Prabhu, 2018).

Table 8. Thermodynamic parameters of AMX adsorption on sepiolite-rich dolomite

$\Delta S°_{ads}$ (kJ/(mol·K))	$\Delta H°_{ads}$ (kJ/mol)	$\Delta G°_{ads}$ (kJ/mol)			
		298 K	308 K	318 K	328 K
0.030	−5.86	−14.44	−15.24	−15.81	−15.19

The adsorption kinetics, adsorption isotherms, and thermodynamic parameters indicate that AMX molecules adsorb onto sepiolite-rich dolomite by a combination of surface and pore diffusion influenced by the pore size and surface characteristics of sepiolite-rich dolomite. The adsorption of AMX onto a dolomite-rich sepiolite surface can be quantified by calculating the cross-sectional area of the AMX molecule in Å²/molecule using Eq. 7 (Özdemir et al., 2007).

$$\text{Cross-sectional area} = 10^{20}/(\Gamma_{max} \times A) \quad (7)$$

Here, A indicates the Avogadro number (6.02×10^{23}), and Γ_{max} represents the maximum adsorption density. Using the experimental Γ_{max} value, the effective surface area occupied per AMX molecule on the sepiolite-rich dolomite was determined to be 9 776 Å²/molecule. As expressed in Table 1, The area of the AMX molecule is approximately 161 Å² (Table 1). It was inferred that AMX molecules occupy about 1.65% of the total surface area of sepiolite-rich dolomite. This low surface coverage suggests that adsorption sites are not fully saturated, supporting the applicability of the Freundlich model, which assumes heterogeneous surface energies and multilayer adsorption (Saadi et al., 2015), indicating that both surface adsorption and pore diffusion with negligible internal mass transfer resistance (Roque-Malherbe, 2007; Šljivić et al., 2011) contribute to the overall adsorption mechanism. Therefore, this may be due to changes in the surface charges of sepiolite-rich dolomite and AMX, which present different molecular forms as a function of the pH range (Fig. 9).

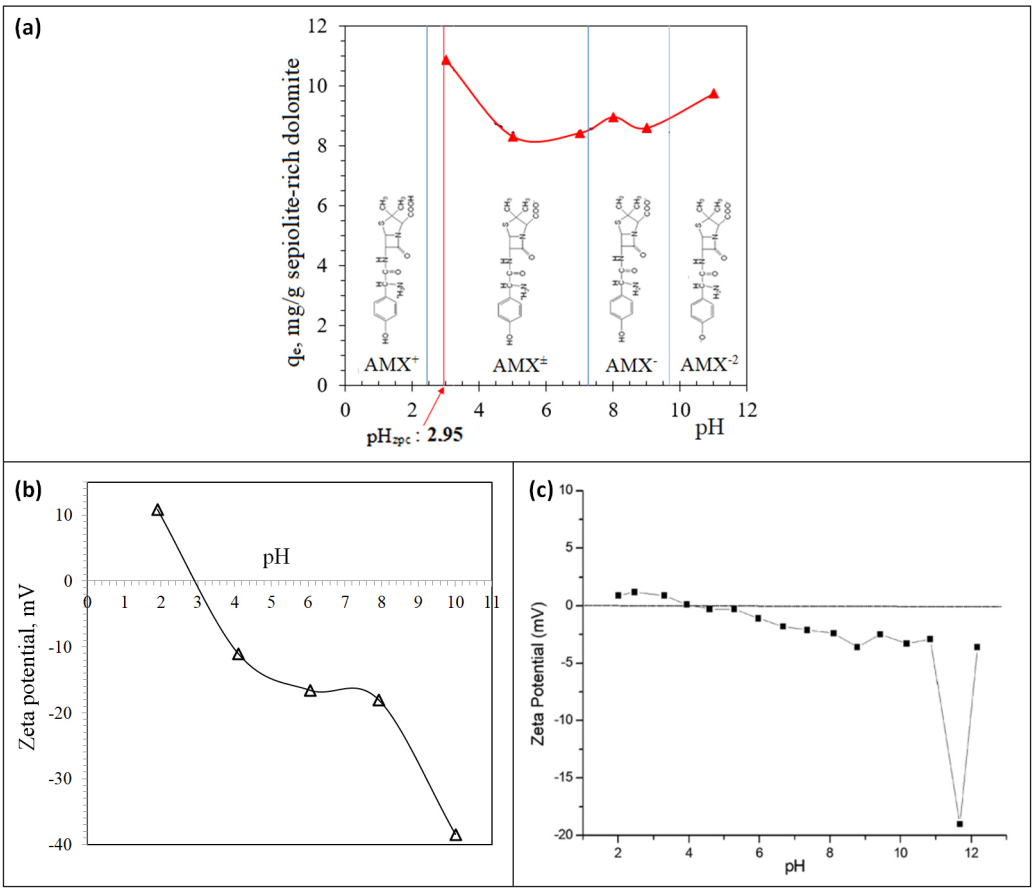

Figure 9. (a) The change in AMX adsorption by sepiolite-rich dolomite at 25°C as a function of solution pH (C_0 = 50 mg/L, T = 25°C, m = 1 g/L, t = 30 min), (b) the pH_{zpc} of sepiolite-rich dolomite, and (c) the pH_{zpc} of the AMX (Zeta potential curve of amoxicillin trihydrate adapted from the article of Novo et al. (2022))

Adsorption mechanism

AMX has a molecular structure including a lactam ring and aromatic group in its chemical form; because it contains different functional groups, the molecular charge of AMX varies depending on the pH (Fig. 9a), and it can exist in three various forms in solution: cationic form (AMX^+) at pH < 2.4, neutral form ($AMX^\pm$) at pH between 2.4 and 7.4, and anionic form (AMX^-, AMX^{2-}) at pH > 7.4 (De Marco et al., 2017). These forms affect the adsorption of AMX onto sepiolite-rich dolomite, which is related to both the molecular form of AMX (Fig. 9a) and the surface electric charge of sepiolite-rich dolomite (Fig. 9b), where the pH_{zpc} of sepiolite-rich is 2.95. As shown in Fig. 9a, the adsorbed amount of AMX (q_e) does not vary significantly with pH, except for a slight increase at pH 3 and 11. The pKa values of AMX-related variations in surface charges of AMX (Aranda and Rivas, 2022) and sepiolite-rich dolomite may explain the interrelation between the solution pH and the adsorption capacity of AMX. In acidic environments at pH 3, sepiolite-rich dolomite is slightly negatively charged, and AMX is positively charged. When Fig. 9a is examined, the highest AMX adsorption capacity is achieved at pH 3, where sepiolite-rich dolomite is slightly negatively charged, and AMX is positively charged. Similar observations were noted in the studies conducted by Mohammed et al. (2024), Rashid et al. (2002), and Pandey et al. (2021). In this case, electrostatic interactions and cation exchange are strong between the sepiolite-rich dolomite and AMX (Thiebault, 2019; Oliveira et al., 2018) resulting in high adsorption efficiency, as indicated by the absence of any difference in the intensity of the Si-O stretching peaks corresponding to the Si-O-Si stretching vibration in the tetrahedral sheet and a slight increase in the position of the peak (1 022 cm^{-1}) seen in the spectrum at 1 020 cm^{-1} after amoxicillin adsorption presented in Fig. 4b (Liu et al., 2024). Putra et al. (2009) reported that the protonation of functional groups of both amoxicillin and bentonite at low pH increased the adsorption capacity of clay minerals. Therefore, the medium needs to be acidified to reach maximum removal efficiency. Furthermore, hydrogen bonds can still form between the hydroxyl groups on sepiolite-rich dolomite and the amide groups on AMX (Eq. 8), corresponding to the shift of the Mg_3OH peaks in the 3 564–3 686 cm^{-1} region. A similar adsorption mechanism involving hydrogen bonding between the hydroxyl group of an adsorbent and the amide group of a molecule was also described by Eniola et al. (2019) for sulfamethoxazole. At pH 5–9, both sepiolite-rich dolomite and AMX are negatively charged. In this case, electrostatic repulsion forces are strong but not enough to prevent the adsorption process. A possible reason is that the ion exchange mechanism between the Mg^{2+} and Ca^{2+} ions on sepiolite-rich dolomite and the protonated carboxyl and amine groups in the AMX is significant (Zha et al., 2013). This is evidenced by the SEM/EDX data obtained before and after AMX adsorption (Fig. 10), which show a decrease in the Ca^{2+} and Mg^{2+} ratios of sepiolite-rich dolomite after AMX adsorption. The Ca^{2+} ratio of 21.85% for sepiolite-rich dolomite before AMX adsorption decreased to 9.37% after AMX adsorption. In addition, a decrease occurred in the Mg^{2+} content of sepiolite after AMX adsorption. The Mg^{2+} ratio, which was 13.30% on the average before AMX adsorption, decreased to 9.49% after AMX adsorption. Moreover, at pH 11, the adsorption of AMX is further enhanced by the interactions of its deprotonated phenolic groups (Míguez-González et al., 2023) with Mg^{2+} ions on the sepiolite surface through coordination bonds, potentially mediated by zeolitic/bound water molecules associated with the Mg^{2+} (Eq. 9). These interactions cause a shift from 1654 cm^{-1}, corresponding to the OH-stretching vibration, to 1645 cm^{-1} in the FTIR spectrum.

$$\equiv Si{-}OH + AMX = \equiv Si{-}O^- + AMX{-}OH \quad (8)$$

$$\equiv Mg(OH_2) + AMX^{2-} = \equiv Mg(OH_2)(AMX)^{2-} \quad (9)$$

In addition, amphoteric AMX molecules interact with –COOH and –OH proton donor and $–NH_2$ proton acceptor groups and functional groups in the octahedral and tetrahedral structural forms of sepiolite-rich dolomite, which facilitates the diffusion of AMX molecules into the active adsorption sites of sepiolite-rich dolomite's macro-channels and pores on the outer surfaces, which enable the easy adsorption of organic structures whose molecular size and shape are very close to the dimensions of open channels (Imanipoor et al., 2020). The diffusion rate is controlled mainly by the molecular size of AMX and the well-developed pore structure/channel openings of sepiolite-rich dolomite. The molecular size of AMX at pH values from 2.74 to 9.63, determined by Pezoti et al. (2016) using ChemBio 3D software (Version 11.0.1), varies between 12.9 and 15.9 Å., which is relatively smaller than the average

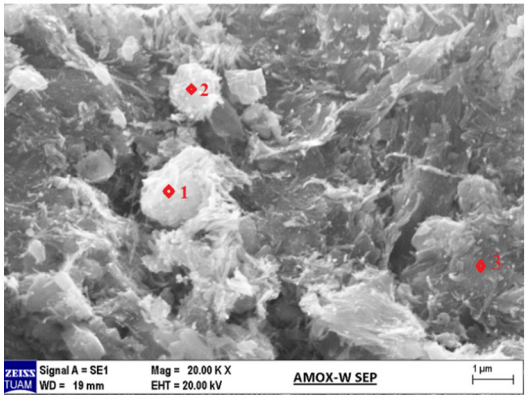

Sepiolite-rich dolomite + AMX	O	Si	Mg	Ca	Al
Pt-1	60.78	8.13	8.61	9.50	-
Pt-2	59.08	12.48	10.94	8.61	-
Pt-3	54.96	7.97	8.92	10.01	0.06
$\sum_{n=1}^{n} P_t/n$	58.27	9.53	9.49	9.37	0.02

Figure 10. Representative SEM image and EDX analysis of sepiolite-rich dolomite after AMX adsorption

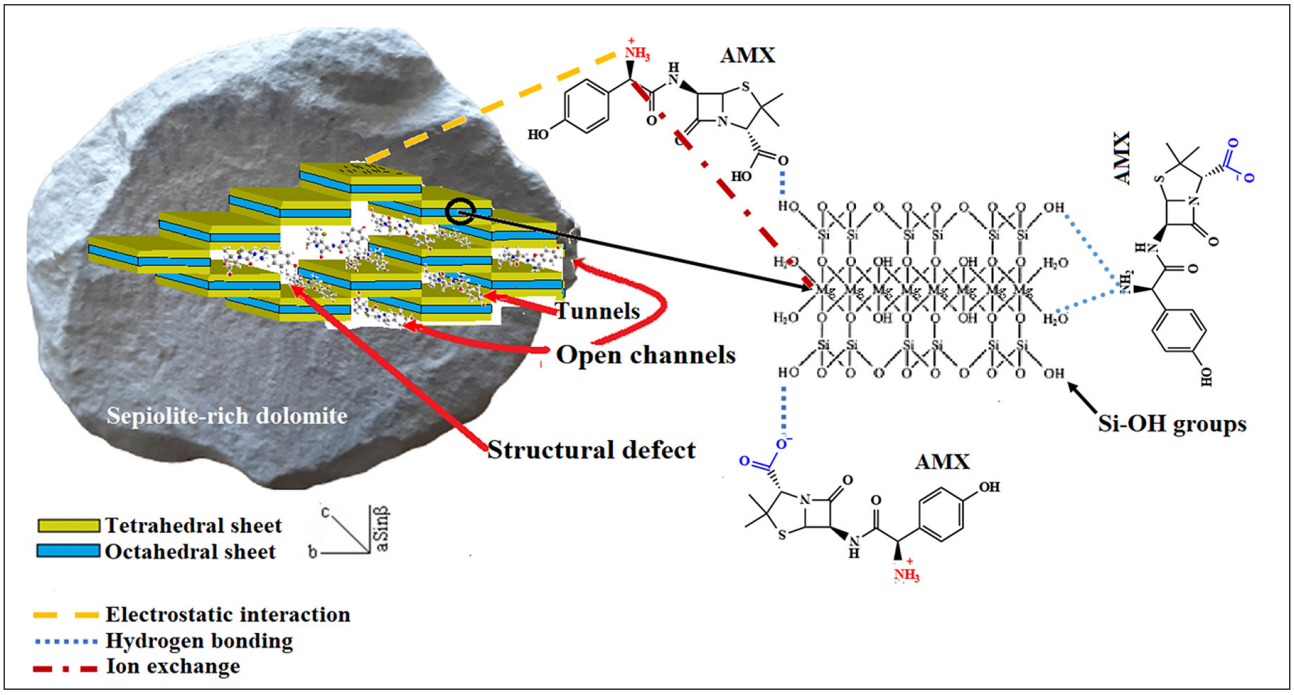

Figure 11. Schematic representation of possible sorption mechanism of AMX to sepiolite-rich dolomite

pore diameter of about 77.6 Å (pore volume of 0.251 cm^3/g) for sepiolite-rich dolomite. Therefore, AMX molecules can easily diffuse and enter into macro pores/channels of sepiolite-rich dolomite, interacting with the active adsorption sites. The active sites contain exchangeable Ca^{2+}/Mg^{2+} ions and H_2O molecules in zeolite-like channels. Si-OH structures found on the basal surfaces of sepiolite-rich dolomite and open channel defects (OCD) structures caused by the very high H_2O content (31.66%) of sepiolite-rich dolomite. Krekeler and Guggenheim (2008) found that imperfections are general and identified two properties: (i) deficient polysomes or an OCD with a cross-sectional space of about 1 000 $Å^2$ (large enough for AMX diffusion with a molecular area of 161 $Å^2$) and (ii) an area where increased crystallization forms a three-sided enclosure and where an OCD structure may evolve with increased crystallization. They suggested that the entity of OCD structures in sepiolite-rich dolomite with a specific surface space of 141 m^2/g creates wide channels that allow zeolitic H_2O molecules to be more mobile throughout exchange with organic molecules and thus account for the strong sorption of the large AMX molecules into sepiolite-rich dolomite. The possible adsorption mechanism for AMX adsorption by sepiolite-rich dolomite is displayed in Fig. 11.

CONCLUSION

The adsorptive removal of the antibiotic drug amoxicillin (AMX) from an aqueous environment using sepiolite-rich dolomite as an inexpensive and natural adsorbent was experimentally studied as a function of temperature, time, AMX concentration, and pH. The sepiolite-rich dolomite also has a mesoporous form with a pore volume of 0.251 cm^3/g and a mean pore diameter of approximately 77.6 Å. Under optimal conditions, the maximum adsorption capacity of AMX on sepiolite-rich dolomite was 123.46 mg/g, comparable to or higher than those reported for other low-cost adsorbents. Adsorption was mainly governed by electrostatic interactions, ion exchange, and pore-filling mechanisms. The Freundlich isotherm model and pseudo-second-order kinetic model were the best fits for the AMX adsorption on sepiolite-rich dolomite. The mechanism of AMX adsorption onto sepiolite-rich dolomite was elucidated by different analytical methods including SEM+EDX and FTIR. The FTIR spectra displayed that the major functional groups related to the AMX adsorption were Si-OH, Mg-OH, and Mg-OH_2 on sepiolite-rich dolomite. The SEM+EDX images showed that the surface morphology and elemental composition of sepiolite-rich dolomite changed upon AMX adsorption. Moreover, the structures of open channel defects (OCD) caused by the very high H_2O content (31.66%) of sepiolite-rich dolomite facilitated the AMX diffusion into its active sites.

AUTHOR CONTRIBUTIONS

E Sabah: conceptualization, methodology, writing and editing, and supervision. N Bilgin: methodology, data curation, and investigation. E Bulut: formal analysis, data curation, and writing.

ORCID

Eyüp Sabah
https://orcid.org/0000-0002-5225-0891

REFERENCES

ABBAS M and TRARI M (2024) Removal of amoxicillin from wastewater onto activated carbon: optimization of analytical parameters by response surface methodology. *Dose-Response* **22** (3). https://doi.org/10.1177/15593258241271655

AL-GHEETHI AAS and ISMAIL N (2014) Biodegradation of pharmaceutical wastes in treated sewage effluents by *Bacillus subtilis* 1556WTNC. *Environ. Process.* **1** 459–481. https://doi.org/10.1007/s40710-014-0034-6

ALKAN M, DEMIRBAŞ O and DOGAN M (2007) Adsorption kinetics and thermodynamics of an anionic dye onto sepiolite. *Micropor. Mesopor. Mater.* **101** 388–396. https://doi.org/10.1016/j.micromeso.2006.12.007

ALVER BE, SAKICI M, YÖRÜKOĞULLARI E, YILMAZ Y and GÜVEN M (2008) Thermal behavior and water adsorption of natural and modified sepiolite having dolomite from Turkey. *J. Ther. Anal. Calorim.* **94** (3) 835-840. https://doi.org/10.1007/s10973-008-9032-0

ANASTOPOULOS I, PASHALIDIS I, ORFANOS AG, MANARIOTIS ID, TATARCHUK T, SELLAOUI L, BONILLA-PETRICIOLET A, MITTAL A and NÚNEZ-DELGADO A (2020) Removal of caffeine. nicotine and amoxicillin from (waste) waters by various adsorbents. a review. *J. Environ. Manage.* **261** 1–9. https://doi.org/10.1016/j.jenvman.2020.110236

ARANDA FL and RIVAS BL (2022) Removal of amoxicillin through different methods, emphasizing removal by biopolymers and its derivatives. An overview. *J. Chil. Chem. Soc.* **67** (3) 5643-5654. https://doi.org/10.4067/S0717-97072022000305643

BAGHAPOUR MA, SHIRDARREH MR and FARAMARZIAN M (2014) Degradation of amoxicillin by bacterial consortium in a submerged biological aerated filter: volumetric removal modeling. *J. Health Sci. Surveill. Syst.* **2** 15-25.

BALARAK D, ZAFARIYAN M and SIDDIQUI S (2020) Investigation of adsorptive properties of surfactant modified sepiolite for removal of ciprofloxacin. *Int. J. Life Sci. Pharma Res.* **10** (3) P12-19. https://doi.org/10.22376/ijpbs/lpr.2020.10.3.P12-19

BASTIDA J, KOJDECKI MA, PARDO P and AMORÓS P (2006) X-ray diffraction line broadening on vibrating dry-milled Two Crows sepiolite. *Clays Clay Miner.* **54** (3) 390-401. https://doi.org/10.1346/CCMN.2006.0540310

BECKER D, GIUSTINA SVD, RODRIGUEZ-MOZAZ S, SCHOEVAART R, BARCELÓ D, DE CAZES M, BELLEVILLE M, SANCHEZ-MARCANO J, DE GUNZBURG J, COUILLEROT O, VÖLKER J, OEHLMANN J and WAGNER M (2016) Removal of antibiotics in wastewater by enzymatic treatment with fungal laccase - degradation of compounds does not always eliminate toxicity. *Bioresour. Technol.* **219** 500-509. https://doi.org/10.1016/j.biortech.2016.08.004

BELAISSA Y, SAIB F and TRARI M (2022) Removal of amoxicillin in aqueous solutions by a chemical activated carbon derived from jujube nuts: adsorption behaviors: kinetic and thermodynamic studies. *React. Kinet. Mech. Catal.* **135** 1011–1030. https://doi.org/10.1007/s11144-022-02159-0

BOSHIR AHMED M, ZHOU JL, HAO NGO H and GUO W (2015) Adsorptive removal of antibiotics from water and wastewater: Progress and challenges. *Sci. Total Environ.* **532** 112-126. https://doi.org/10.1016/j.scitotenv.2015.05.130

BUDYANTO S, SOEDJONO S, IRAWATY W and INDRASWATI N (2008) Studies of adsorption equilibria and kinetics of amoxicillin from simulated wastewater using activated carbon and natural bentonite. *J. Environ. Protect. Sci.* **2** 72–80.

CHAYID MA and AHMED MJ (2015) Amoxicillin adsorption on microwave prepared activated carbon from *Arundo donax* Linn: Isotherms, kinetics, and thermodynamics studies. *J. Environ. Chem. Eng.* **3** 1592–1601. https://doi.org/10.1016/j.jece.2015.05.021

CHUAICHAM C, PAWAR R and SASAKI K (2019) Dye-sensitized photocatalyst of sepiolite for organic dye degradation. *Catalysis* **9** (3) 235. https://doi.org/10.3390/catal9030235

DABROWSKI A (1986) Langmuir-Freundlich Equation and its application for describing adsorption from non-ideal binary liquid mixtures on heterogeneous solid surfaces. *Z. Phys. Chem.* **267** (1) 494–506. https://doi.org/10.1515/zpch-1986-26759

DE FRANCO MAE, DE CARVALHO CB, BONETTO MM, SOARES RDP and FÉRIS LA (2017) Removal of amoxicillin from water by adsorption onto activated carbon in batch process and fixed bed column: kinetics. isotherms. experimental design and breakthrough curves modelling. *J. Clean. Prod.* **161** 947–956. https://doi.org/10.1016/j.jclepro.2017.05.197.

DE MARCO BA, NATORI JSH, FANELLI S, TÓTOLI EG and SALGADO HRN (2017) Characteristics, properties and analytical methods of amoxicillin: a review with green approach. *Crit. Rev. Anal. Chem.* **47** (3) 267–277. https://doi.org/10.1080/10408347.2017.1281097

DHARMARATHNA SP and PRIYANTHA N (2024) Investigation of boundary layer effect of intra-particle diffusion on methylene blue adsorption on activated carbon. *Energ. Nexus* **14** 100294. https://doi.org/10.1016/j.nexus.2024.100294

ENIOLA JO, KUMAR R and BARAKAT MA (2019) Adsorptive removal of antibiotics from water over natural and modified adsorbents. *Environ. Sci. Pollut. Res.* **26** 34775–34788. https://doi.org/10.1007/s11356-019-06641-6

FIGUEIREDO VV, VIANNA ELF, LIMA BS, JESUS TCL, GARCÍA-VILLÉN F, BERTOLINO LC, SPINELLI LS and VISERAS C (2024) Brazilian palygorskite as an alternative to commercial adsorbents for methylene blue: A discussion about composition, morphology and pore profile. *Micropor. Mesopor. Mater.* **366** 112957. https://doi.org/10.1016/j.micromeso.2023.112957

FOO KY and HAMEED BH (2010) Insights into the modeling of adsorption isotherm systems. *Chem. Eng. J.* **156** (1) 2–10. https://doi.org/10.1016/j.cej.2009.09.013

GENÇ N and DOGAN EC (2015). Adsorption kinetics of the antibiotic ciprofloxacin on bentonite, activated carbon, zeolite, and pumice. *Desalin. Water Treat.* **53** (3) 785–793. https://doi.org/10.1080/19443994.2013.842504

GHOLAMI M, MIRZAEI R, KALANTARY RR, SABZALI A and GATEI F (2012) Performance evaluation of reverse osmosis technology for selected antibiotics removal from synthetic pharmaceutical wastewater. *J. Environ. Health Sci. Eng.* **9** 1–10. https://doi.org/10.1186/1735-2746-9-19

GILES GH and SMITH D (1974) A general treatment and classification of the solute adsorption isotherm. I. Theoretical. *J. Colloid Interface Sci.* **47** 755–765. https://doi.org/10.1016/0021-9797(74)90252-5

GOMES MP (2024) The Convergence of antibiotic contamination, resistance, and climate dynamics in freshwater ecosystems. *Water* **16** (18) 2606. https://doi.org/10.3390/w16182606

GÜNDÜZ F and BAYRAK B (2017) Biosorption of malachite green from an aqueous solution using pomegranate peel: equilibrium modelling, kinetic and thermodynamic studies. *J. Mol. Liq.* **243** 790–798. https://doi.org/10.1016/j.molliq.2017.08.095

GÜNGÖRDÜ A (2018) Removal of antibiotic from wastewater by advanced treatment methods. PhD thesis, Anadolu University (in Turkish).

HINZ C (2001) Description of sorption data with isotherm equations. *Geoderma* **99** 225–243. https://doi.org/10.1016/S0016-7061(00)00071-9

HOMAYOONFAL M and MEHRNIA MR (2014) Amoxicillin separation from pharmaceutical solution by ph sensitive nanofiltration membranes. *Sep. Purif. Technol.* **130** 74–83. https://doi.org/10.1016/j.seppur.2014.04.009

HUGHES SR, KAY P and BROWN LE (2016) Impact of anti-inflammatories, beta-blockers and antibiotics on leaf litter breakdown in freshwaters. *Environ. Sci. Pollut. Res.* **23** 3956–3962. https://doi.org/10.1007/s11356-015-5798-3

HUSSAINI SR and DVORKIN J (2021) Specific surface area versus porosity from digital images: High-porosity granular samples. *J. Petrol. Sci. Eng.* **206** 108961. https://doi.org/10.1016/j.petrol.2021.108961

IMANIPOOR J, MOHAMMADI M, DINARI M and EHSANI MR (2020) Adsorption and desorption of amoxicillin antibiotic from water matrices using an effective and recyclable MIL-53(Al) metal-organic framework adsorbent. *J. Chem. Eng. Data* **66** (1) 389–403. https://doi.org/10.1021/acs.jced.0c00736

JIN X, ZHA S, LI S and CHEN Z (2014) Simultaneous removal of mixed contaminants by organoclays-amoxicillin and Cu(II) from aqueous solution. *Appl. Clay Sci.* **102** 196–201. https://doi.org/10.1016/j.clay.2014.09.040

JONES BF and GALAN E (1988) Sepiolite and palygorskite. In: Bailey SW (ed.) *Hydrous Phyllosilicates*. Mineralogical Society of America, Michigan. 631–674.

KAM SK and LEE MG (2018) Adsorption characteristics of antibiotics amoxicillin in aqueous solution with activated carbon prepared from waste citrus peel. *Appl. Chem. Eng.* **29** 369–375. https://doi.org/10.14478/ace.2018.1015

KARAKAYA N, ÇELIK KARAKAYA M, TEMEL A, KÜPELI Ş and TUNOĞLU C (2004) Mineralogical and chemical characterization of sepıolite occurrences at Karapınar (Konya basın, Turkey). *Clays Clay Miner.* **52** 495–509. https://doi.org/10.1346/CCMN.2004.0520410

KHUMALO SM, BAKARE BF and RATHILAL S (2023) Simultaneous sorption of ciprofloxacin and amoxicillin on chitosan composites from aqueous solutions: kinetics and isotherms. In: *International Conference on "Chemical, Biological and Environmental Engineering" (JCBEE-23)*, 16–17 November 2023, Johannesburg.

KIDAK R and DOĞAN Ş (2018) Medium-high frequency ultrasound and ozone based advanced oxidation for amoxicillin removal in water. *Ultrason. Sonochem.* **40** 131–139. https://doi.org/10.1016/j.ultsonch.2017.01.033

KREKELER MPS and GUGGENHEIM S (2008) Defects in microstructure in palygorskite–sepiolite minerals: a transmission electron microscopy (TEM) study. *Appl. Clay. Sci* **39** 98–105. https://doi.org/10.1016/j.clay.2007.05.001

LESCANO L, CASTILLO L, MARFIL S, BARBOSA S and MAIZA P (2014) Alternative methodologies for sepiolite defibering. *Appl. Clay Sci.* **95** 378–382. https://doi.org/10.1016/j.clay.2014.05.001

LI G, HE J, WANG D, MENG P and ZENG M (2014) Optimization and interpretation of O3 and O3/H2O2 oxidation processes to pretreat hydrocortisone pharmaceutical wastewater. *Environ. Technol.* **36** (8) 1026–1034. https://doi.org/10.1080/09593330.2014.971885

LIMOUSY L, GHOUMA I, OUEDERNI A and JEGUIRIM M (2017) Amoxicillin removal from aqueous solution using activated carbon prepared by chemical activation of olive stone. *Environ. Sci. Pollut. Res.* **24** 9993–10004. https://doi.org/10.1007/s11356-016-7404-8

LIU Y, WANG F, CHEN X, ZHANG J and GAO B (2015) Cellular responses and biodegradation of amoxicillin in *Microcystis aeruginosa* at different nitrogen levels. *Ecotoxicol. Environ. Saf.* **111** 138–145. https://doi.org/10.1016/j.ecoenv.2014.10.011

LIU Z, JIANG Y, HE R, WU J, ZHANG X, HUANG K and WU Y (2024) Adsorption retention of spiramycin in agricultural calcareous loess soils: Assessing the impact of influential factors and mechanisms. *Water Air Soil Pollut.* **235** 491. https://doi.org/10.1007/s11270-024-07312-0

LÓPEZ-LUNA J, RAMÍREZ-MONTES LE, MARTINEZ-VARGAS S, MARTÍNEZ AI, MIJANGOS-RICARDEZ OF, GONZÁLEZ-CHÁVEZ MCA, CARRILLO-GONZÁLEZ R, SOLÍS-DOMÍNGUEZ FA, CUEVAS-DÍAZ MC and VÁZQUEZ-HIPÓLITO V (2019) Linear and nonlinear kinetic and isotherm adsorption models for arsenic removal by manganese ferrite nanoparticles. *SN Appl. Sci.* **1** 950. https://doi.org/10.1007/s42452-019-0977-3

MAIA GS, ANDRADE JR, OLIVEIRA MF, VIEIRA MGA and DA SILVA MGC (2017) Affinity studies between drugs and clays as adsorbent material. *Chem. Eng. Trans.* **57** 583–588. https://doi.org/10.3303/CET1757098

MANE PV, REGO RM, YAP PL, LOSIC D and KURKURI MD (2024) Unveiling cutting-edge advances in high surface area porous materials for the efficient removal of toxic metal ions from water. *Prog. Mater. Sci.* **146** 101314. https://doi.org/10.1016/j.pmatsci.2024.101314

MANSOURI H, CARMONA RJ, GOMIS-BERENGUER A, SOUISSI-NAJAR S, OUEDERNI A and ANIA CO (2015) Competitive adsorption of ibuprofen and amoxicillin mixtures from aqueous solution on activated carbons. *J. Colloid Interf. Sci.* **449** 252–260. https://doi.org/10.1016/j.jcis.2014.12.020.

MÍGUEZ-GONZÁLEZ A, CELA-DABLANCA R, BARREIRO A, RODRÍGUEZ-LÓPEZ L, RODRÍGUEZ-SEIJO A, ARIAS-ESTÉVEZ M, NÚÑEZ-DELGADO A, FERNÁNDEZ-SANJURJO MJ, CASTILLO-RAMOS V and ÁLVAREZ-RODRÍGUEZ E (2023) Adsorption of antibiotics on bio-adsorbents derived from the forestry and agro-food industries. *Environ. Res.* **233** 116360. https://doi.org/10.1016/j.envres.2023.116360

MOHAMMADI A, KAZEMIPOUR M, RANJBAR H, WALKER RB and ANSARI M (2014) Amoxicillin removal from aqueous media using multi- walled carbon nanotubes. *Fuller. Nanotub. Car. N.* **23** 165–169. https://doi.org/10.1080/1536383X.2013.866944

MOHAMMED AA and ALNASRAWI FA (2024) Adsorption of Pb^{2+} ions by MgCuAl-layered double hydroxides@montmorillonite nanocomposite in batch and circulated fluidized bed system: Hydrodynamic and mass transfer studies. *J. Water Process Eng.* **63** 105519. https://doi.org/10.1016/j.jwpe.2024.105519

MOHAMMED AK, SAADOON SM, ABD ALI ZT, RASHID IM and AL SBANI NH (2024) Removal of amoxicillin from contaminated water using modified bentonite as a reactive material. *Heliyon* **10** (3) e24916. https://doi.org/10.1016/j.heliyon.2024.e24916

NARAYANAN N, MATHERS AJ, WENZLER E, MOORE NM, GISKE CG, MENDES RE and EDELSTEIN PH (2024) Amoxicillin-clavulanate breakpoints against *Enterobacterales*: rationale for revision by the Clinical and Laboratory Standards Institute. *Clin. Infect. Dis.* **79** (2) 516–523. https://doi.org/10.1093/cid/ciae201

NASROLLAHI N, VATANPOUR V and KHATAEE A (2022) Removal of antibiotics from wastewaters by membrane technology: Limitations, successes, and future improvements. *Sci. Total Environ.* **838** (1) 156010. https://doi.org/10.1016/j.scitotenv.2022.156010

NIERO G, RODRIGUES CA, ALMERINDO GI, CORREA AXR, GASPARETO P, FEUZER-MATOS AJ, SOMENSI CA and RADETSKI CM (2021) Using basic parameters to evaluate adsorption potential of alternative materials: example of amoxicillin adsorption by activated carbon produced from termite bio-waste. *J. Environ. Sci. Health A Tox. Hazardous Subst. Environ. Eng.* **56** 32–43. https://doi.org/10.1080/10934529.2020.1835125

NOVO BL, GOMES DA SILVA FAN, BERTOLINO LC and YOKOYAMA L (2022) Amoxicillin trihydrate characterization and investigative adsorption using a Brazilian montmorillonite. *Revista Materia.* **27** (3). https://doi.org/10.1590/1517-7076-rmat-2022-0109

OLIVEIRA T, FERNANDEZ E, FOUGÈRE L, DESTANDAU E, BOUSSAFIR M, SOHMIYA M, SUGAHARA Y and GUÉGAN R (2018) Competitive association of antibiotics with a clay mineral and organoclay derivatives as a control of their lifetimes in the environment. *ACS Omega* **3** (11) 15332–15342. https://doi.org/10.1021/acsomega.8b02049

ÖZDEMİR O, ÇINAR M, SABAH E, ARSLAN F and ÇELİK MS (2007) Adsorption of anionic surfactants onto sepiolite. *J. Hazardous Mater.* **147** (1–2) 625–632. https://doi.org/10.1016/j.jhazmat.2007.01.059

ÖZER ET (2020) Removal of amoxicillin in aqueous solution by an activated carbon: kinetic and equilibrium studies. *EJOSAT* **18** 833–839. https://doi.org/10.31590/ejosat.697040

PALMA E, ELLISON L, MEZA E and GRIKO Y (2016) Calorimetric evaluation of amoxicillin stability in aqueous solutions. *Mathews J. Pharm. Sci.* **2** (1) 1–8.

PANDEY P, SHANKAR A, BINEY M and SAINI VK (2021) Enhancement in amoxicillin adsorption and regeneration properties of SBA-15 after surface modification with polyaniline. *Colloid Interf. Sci. Commun.* **43** 100432. https://doi.org/10.1016/j.colcom.2021.100432

PERINI JAL, TONETTI AL, VIDAL C, MONTAGNER CC and NOGUEIRA RFP (2018) Simultaneous degradation of ciprofloxacin, amoxicillin, sulfathiazole and sulfamethazine, and disinfection of hospital effluent after biological treatment via photo-Fenton process under ultraviolet germicidal irradiation. *Appl. Catal. B Environ.* **224** 761–771. https://doi.org/10.1016/j.apcatb.2017.11.021

PEZOTI O, CAZETTA AL, BEDIN KC, SOUZA LS, MARTINS AC, SILVA TL, SANTOS JÚNIOR O, VISENTAINER JV and ALMEIDA VC (2016) NaOH-activated carbon of high surface area produced from guava seeds as a high-efficiency adsorbent for amoxicillin removal: kinetic. isotherm and thermodynamic studies. *Chem. Eng. J.* **288** 778–788. https://doi.org/10.1016/j.cej.2015.12.042

POURETEDAL HR and SADEGH N (2014) Effective removal of amoxicillin, cephalexin, tetracycline and penicillin G from aqueous solutions using activated carbon nanoparticles prepared from vine wood. *J. Water Process. Eng.* **1** 64–73. https://doi.org/10.1016/j.jwpe.2014.03.006

PRABHU PP and PRABHU B (2018) A Review on removal of heavy metal ions from waste water using natural/modified bentonite. *MATEC Web of Conferences.* **144** 02021. https://doi.org/10.1051/matecconf/201814402021

PUTRA EK, PRANOWO R, SUNARSO J, INDRASWATI N and ISMADJI S (2009) Performance of activated carbon and bentonite for adsorption of amoxicillin from wastewater: mechanisms, isotherms and kinetics. *Water Res.* **43** 2419–2430. https://doi.org/10.1016/j.watres.2009.02.039

RASHID SA, NAIFE TM and KURJI BM (2022) Removal of amoxicillin from wastewater by adsorption onto activated carbon prepared from sunflower seed hulls. *Desalin. Water Treat.* **276** 93–103. https://doi.org/10.5004/dwt.2022.28945

ROQUE-MALHERBE RMA (2007) *Adsorption and Diffusion in Nanoporous Materials* (1st edn). CRC Press, Boca Raton. 288 pp.

SAADİ R, SAADİ Z, FAZAELİ R and ELMİ FARD N (2015) Monolayer and multilayer adsorption isotherm models for sorption from aqueous media. *Korean J. Chem. Eng.* **32** (5) 787–799. https://doi.org/10.1007/s11814-015-0053-7

SABAH E and OUKI S (2017) Mechanistic insight into pyrene removal by natural sepiolites. *Environ. Sci. Pollut. Res.* **24** 21680–21692. https://doi.org/10.1007/s11356-017-9524-1

SAHMOUNE MN (2019) Evaluation of thermodynamic parameters for adsorption of heavy metals by green adsorbents. *Environ. Chem. Lett.* **17** 697–704. https://doi.org/10.1007/s10311-018-00819-z

SELLAOUI L, LIMA EC, DOTTO GL and LAMINE AB (2017) Adsorption of amoxicillin and paracetamol on modified activated carbons: Equilibrium and positional entropy studies. *J. Mol. Liq.* **234** 375–381. https://doi.org/10.1016/j.molliq.2017.03.111

SILVA BS, RIBEIRO MCB, RAMOS B and PEIXOTO ALC (2022) Removal of amoxicillin from processing wastewater by ozonation and UV-aided ozonation: Kinetic and economic comparative study. *Water* **14** (20) 3198. https://doi.org/10.3390/w14203198

ŠLJİVİĆ M, SMİČİKLAS I, PLEĆAŠ I and PEJANOVİĆ S (2011) The role of external and internal mass transfer in the process of Cu^{2+} removal by natural mineral sorbents. *Environ. Technol.* **32** (19) 933–943. https://doi.org/10.1080/09593330.2010.521952

SONG Y (2018) The adsorption of amoxicillin by mesoporous silica supported polymers. Master's thesis, The State University of New Jersey.

SUÁREZ M, GARCÍA-RIVAS J, GARCÍA-ROMERO E and JARA N (2016) Mineralogical characterization and surface properties of sepiolite from Polatli (Turkey). *Appl. Clay Sci.* **131** 124–130. https://doi.org/10.1016/j.clay.2015.12.032

SUN J, WANG L, LU S, WANG Z, CHEN M, LIANG W, LIN X and LIN X (2022) Environmentally friendly g-C_3N_4/sepiolite fiber for enhanced degradation of dye under visible light. *Molecules* **27** (8) 2464. https://doi.org/10.3390/molecules27082464

THIEBAULT T (2019) Raw and modified clays and clay minerals for the removal of pharmaceutical products from aqueous solutions: State of the art and future perspectives. *Crit. Rev. Environ. Sci. Technol.* **50** (14) 1451–1514. https://doi.org/10.1080/10643389.2019.1663065

UĞURLU M (2009) Adsorption of a textile dye onto activated sepiolite. *Micropor. Mesopor. Mater.* **119** 276–283. https://doi.org/10.1016/j.micromeso.2008.10.024

WALCZYK A, KARCZ R, KRYŚCIAK-CZERWENKA J, NAPRUSZEWSKA BD, DURACZYŃSKA D, MICHALIK A, OLEJNICZAK Z, TOMCZYK A, KLIMEK A, BAHRANOWSKI K and SERWICKA EM (2020) Influence of dry milling on phase transformation of sepiolite upon alkali activation: implications for textural, catalytic and sorptive properties. *Materials* **13** (18) 3936. https://doi.org/10.3390/ma13183936

WANG J and GUO X (2022) Rethinking of the intraparticle diffusion adsorption kinetics model: Interpretation, solving methods and applications. *Chemosphere* **309** 136732. https://doi.org/10.1016/j.chemosphere.2022.136732

WANG X, JING J, ZHOU M and DEWIL R (2023) Recent advances in H_2O_2-based advanced oxidation processes for removal of antibiotics from wastewater. *Chin. Chem. Lett.* **34**(3) 107621. https://doi.org/10.1016/j.cclet.2022.06.044

WU FC, TSENG RL and JUANG RS (2009) Initial behavior of intraparticle diffusion model used in the description of adsorption kinetics. *Chem. Eng. J.* **153** (13) 1–8. https://doi.org/10.1016/j.cej.2009.04.042

WU X, ZHANG Q, LIU C, ZHANG X and CHUNG DDL (2017) Carbon-coated sepiolite clay fibers with acid pre-treatment as low-cost organic adsorbents. *Carbon* **123** 259–272. https://doi.org/10.1016/j.carbon.2017.07.063

XIE J, CHEN T, XING B, LIU H, XIE Q, LI H and WU Y (2016) The thermochemical activity of dolomite occurred in dolomite–palygorskite. *Appl. Clay Sci.* **119** (1) 42–48. https://doi.org/10.1016/j.clay.2015.07.014

YALÇIN H and BOZKAYA O (2004) Ultramafic-rock-hosted vein sepiolite occurrences in the Ankara Ophiolitic Mélange, Central Anatolia, Turkey. *Clays Clay Miner.* **52** (2) 227–239. https://doi.org/10.1346/CCMN.2004.0520209

YANG W, ZHOU Y, SONG J, LI Y and GONG T (2024) A novel approach for preparing sepiolite micron powder based on steam pressure changes. *Materials* **17** 3574. https://doi.org/10.3390/ma17143574

YEO JYJ, AQSHA A, ISMADJI S and SUNARSO J (2024) Adsorption kinetics of amoxicillin, ampicillin, and doripenem on organobentonite. *AIP Conf. Proc.* **3073** 070013. https://doi.org/10.1063/5.0194120

ZHA SX, ZMO Y, JIN X and CHEN Z (2013) The removal of amoxicillin from wastewater using organobentonite. *J. Environ. Manage.* **129** 569–576. https://doi.org/10.1016/j.jenvman.2013.08.032

ZHANG N, LI N, HAN X, ZHANG H, MENG J, ZHOU P and LIANG J (2023) In-situ synthesis of sepiolite-supported ceria nanocrystal composites for efficient removal of aflatoxin B1: Enhanced degradation of mycotoxins in the environment by sepiolite nanofibers. *J. Alloys Compd.* **960** 170800. https://doi.org/10.1016/j.jallcom.2023.170800

ZHANG Q, YE C, ZHOU H, CHEN Y, AO F, LUO Y, YANG W, MA M and CHEN X (2024) Active sites regulation and adsorption performance of Al-pillared bentonite for the removal of lead from aqueous phase. *J. Water Process Eng.* **67** 106274. https://doi.org/10.1016/j.jwpe.2024.106274